

# Interface Energy-driven Indium Whisker Growth on Ceramic Substrates

**Shuai Li**

Southeast University

**Yushuang Liu**

Nanjing Institute of Technology

**Peigen Zhang** (✉ [zhpeigen@seu.edu.cn](mailto:zhpeigen@seu.edu.cn))

Southeast University <https://orcid.org/0000-0002-8969-3100>

**Yan Zhang**

Southeast University

**Chengjie Lu**

Southeast University

**Long Pan**

Southeast University

**Jianxiang Ding**

Anhui University of Technology

**Zhengming Sun**

Southeast University

---

## Research Article

**Keywords:** Indium whiskers, ceramic substrates, interface energy, Ti<sub>2</sub>InC

**Posted Date:** March 3rd, 2021

**DOI:** <https://doi.org/10.21203/rs.3.rs-250820/v1>

**License:**   This work is licensed under a Creative Commons Attribution 4.0 International License.

[Read Full License](#)

---

# Abstract

The mechanism behind spontaneous growth of metal whiskers is essential to develop lead-free whisker mitigation strategy for the sake of long-term reliability of electronics, and has been sought for several decades. However, a consensus about it still lacks, and a host of factors influencing the phenomenon have been investigated, but the role of interface energy has not been paid adequate attention. In this study, the whisker growth propensities of ball-milled  $Ti_2InC/In$  and non-MAX phase  $TiC/In$  and  $SiC/In$  are comparatively studied in the terms of the wettability, thermal behavior and crystal structures. The wetting angles of indium with  $Ti_2InC$ ,  $TiC$ , and  $SiC$  ( $144.4^\circ$ ,  $155.7^\circ$ , and  $142.2^\circ$ , respectively) are large and quite close, indicating the poor wettability between liquid indium and the three ceramics. The thermal behaviors of all the three systems have obvious changes after ball milling. The number density of indium whiskers on ball-milled  $Ti_2InC$  are significantly greater than those on the  $TiC$  and  $SiC$  substrates, which is explained based on interface energy and the crystal structure difference of the ceramic substrates.

## Introduction

Spontaneous growth of low melting point metal whiskers has been a reliability problem in the electronics industry for more than 70 years [1, 2]. Although some models and theories have been proposed, the growth mechanism is still not fully revealed [3, 4]. In addition, various phenomena indicate that the similar whisker grow problems have spread from alloys to other materials, such as thin films, intermetallics, and MAX phase ceramics [5-8].

MAX phases are a family of layered compound with the general formula of  $M_{n+1}AX_n$ , where M is an early transition metal, A is an A-group element, X is C or N and usually,  $n=1-4$  [9-11]. All MAX numbers form by alternatively stacking layers constructed by  $M_6X$  octahedrons and A-atom layers. In their crystal structure, covalent bonds predominate within MX layers and relatively weak metal bonds exist between M and A atoms, which makes MAX grains easy to dissociate along their basal planes when subjected to an external force [12, 13]. Due to the unique structure, MAX has metallic and ceramic properties, and has technological significance for a broad spectrum of applications, such as electrical contacts, heating elements, radiation-resistant components, etc. [14-16].

For the MAX powders synthesized via powder metallurgy, usually the case, it is difficult to be free of residual elemental A [17, 18], and the elemental A has proven to have a relationship with the spontaneous growth of metallic whiskers [19, 20]. The whiskering phenomenon may bring about reliability issues as MAX phases is finding their applications, and in particular when used in delicate electronics [16]. However, the mechanism of whisker growth in MAX has not been clearly unraveled to date.

The metallic whisker growth on MAX phase was first reported by Barsoum et al. in 1999 [21], and by analyzing the XRD patterns of  $Gr_2GaN$  before and after Ga whisker growth, the whisker growth was ascribed to the deintercalation of lattice atoms in  $Cr_2GaN$ , and it was driven by compressive stress originated from oxidization. Soon later, however, the authors provided an alternative interpretation

claiming that the excessive elemental Ga left in Cr<sub>2</sub>GaN was the Ga atom source feeding the Ga whisker growth, and its driving force lay in the interface energy between elemental Ga and the Cr<sub>2</sub>GaN phase [22]. A large number of studies have shown that whiskers grow in a vacuum environment, contradicting to the stress-related growth mechanism and implying some other sources of the driving force [23, 24]. At the same time, vapor-deposited thin films on various substrates are also used to investigate the spontaneous growth of metallic whiskers. Liu et al. [5] grew massive Bi nanowires by depositing Bi on the porous vanadium films. Except for low melting point metal whiskers, Kosinova et al. [25] found Au whiskers grew from thin Au films deposited on glass, and Amram et al. [26] reported that Fe nanowires grew from thin Fe films deposited on the surface of sapphire. These studies all conclude that the non-wetting characteristics between the metal films and the substrates drives the whisker growth. The non-wetting behavior between metal and MAX phases should have a similar effect on the whisker growth as the cases for the metal film deposited on ceramics stated above. However, the role of the interface energy has not been paid much attention as the whiskering phenomenon on MAX phases was investigated [20, 27]. This makes the studies of whisker growth overemphasize the effect of structural particularity of MAX phases [28].

To comprehensively understand the growth mechanism of the whiskering phenomenon on MAX phase system, this work chooses Ti<sub>2</sub>InC as a platform and conducts a comparative study using carbide ceramics TiC and SiC (non-MAX ceramics) to explore the growth behavior and mechanism of indium whiskers. It is found that the interface energy plays a key role for the whisker growth, and the findings would advance the fully uncovering the myth of the metallic whisker growth.

## Experimental Procedures

Ti<sub>2</sub>InC was prepared by pressureless sintering the mixture of Ti (99.00%, 250 mesh, Sinopharm), indium (99.90%, 700 mesh, Zhongxin new materials Co.) and graphite (99.85%, 500 mesh, Sinopharm) powders with a molar ratio of 2:1:0.95 at 1250 °C for 1.5 h. The elemental indium left in the as-synthesized Ti<sub>2</sub>InC was removed by immersing it in dilute nitric acid (1 mol/L, 50 °C) with magnetic stirring (500 r/min) for 6 hours, so as not to affect the subsequent quantitative addition of indium; then the etched Ti<sub>2</sub>InC powder free of elemental indium was collected by centrifugation and drying at 60 °C. The etched Ti<sub>2</sub>InC and indium with a molar ratio of 1:0.1 were mixed for 3 hours in a Tublar mixer, and then the mixture was ball milled in a stainless steel jar with stainless steel balls with a charge ratio of 10:1 at 650 r/min for 1 hour. After ball milling, the mixture was formed a disc-shaped sample (φ=16 mm, 0.5 mm thick) by cold press at 1000 MPa. To compare, TiC (99%, 2-4 μm, Macklin)/0.1In (molar ratio) and SiC (98.5%, 100 μm, Sinopharm)/0.1In (molar ratio) were subjected to the same ball milling and cold pressing treatment, respectively. Table 1 lists the parameters of the samples in detail.

The morphologies of the whiskers and substrates were characterized by scanning electron microscope (SEM, FEI Sirion 200, America) and transmission electron microscope (TEM, FEI Tecnai G2-T20, America), and the thermal behavior of the sample was analyzed by differential scanning calorimetry (DSC, Netzsch

STA449F3, Germany). Contact angle measurements (DataPhysics OCA 25, Germany) were performed to test the wettability.

**Table 1** Sample designations and information about ceramics among them.

Compositions (molar ratio)	Substrate properties	
	Size	Vickers hardness
Ti <sub>2</sub> InC/0.1In	~5 μm	2.60 GPa [29]
TiC/0.1In	2-4 μm	28-35 GPa [30]
SiC/0.1In	100 μm	24-28 GPa [31]

## Results And Discussion

### 3.1 Whisker growth in ceramic/In system

Fig. 1 shows the morphologies of the as-synthesized Ti<sub>2</sub>InC, the as-purchased TiC and SiC, and their morphologies after ball milling. As shown in Fig. 1(a), the as-synthesized Ti<sub>2</sub>InC sample consists of agglomerates (~5 μm) of tiny grains. The as-purchased TiC particles are around 2-4 μm, with a few bigger ones (~10 μm). The as-purchased SiC particles are about 100 μm. Shown in Fig. 1(d-f) are the ball-milled Ti<sub>2</sub>InC, TiC and SiC, respectively. Ti<sub>2</sub>InC particles were obviously reduced to submicron, and the tiny particles agglomerate; however, after milling under same parameters, particles of ~10 μm dominate for both TiC and SiC samples, because the latter two ceramics are much harder than Ti<sub>2</sub>InC, Table 1, and in particular, the size of TiC particles almost remained the same.

After being aged at 140 °C for 12 h, whiskers appeared on all the three samples, as shown in Fig. 2. Fig. 2(b) shows that indium whiskers also have longitudinal and transverse striations, a feature shared with metallic whiskers spontaneously grown on solders, platings and other alloy substrates, such as tin [8, 32, 33], zinc [34], bismuth [35]. Fig. 2(e) together with the magnified image Fig. 2(f) show the high-resolution TEM image of the indium whiskers. The whiskers wear an oxide film of ~10 nanometers, and the film has three distinct lattice orientations, indicating that it is polycrystalline, which is different from the reported amorphous oxides covering the Sn whiskers [24].

Among the three samples, the number density and length of indium whiskers on ball-milled Ti<sub>2</sub>InC are significantly greater than those on the TiC and SiC samples. In Fig. 2(a), the length of the entangled whiskers on Ti<sub>2</sub>InC can reach several micrometers. A few number of polyhedrons on the substrate consists of indium, confirmed by the EDS characterization, which may be related to the stability of indium

in air [36], which makes it difficult for indium to oxidize, leading to the reconstruction of surfaces of the indium growth. Similarly, formation of other low-melting metal polyhedrons, such as tin [37], was also observed. In addition, Liu's research on the growth atmosphere of whiskers found that whiskers can form prismatic whiskers surrounded by specific faces in a non-oxidizing atmosphere [38], which shares the same mechanism to the formation of the indium polyhedrons in this work.

The difference in particle size distribution of the samples is mainly determined by the characteristics of the ceramics themselves. In particular,  $\text{Ti}_2\text{InC}$  has a nanolaminate structure, being easily delaminated along its basal planes, while  $\text{TiC}$  and  $\text{SiC}$  have strong covalent bonds and have extremely high hardness, resulting in a huge resistance to milling. The sum of the interface area depends on the size of the particles in the samples and smaller particles have more interfaces with indium after milling, meaning more energy stored. The interface energy would provide driving force for whisker growth.

## 3.2 Whisker growth mechanism driven by interface energy

To measure the wettability of indium with the three ceramic substrates, dense ceramic samples were prepared via SPS and were polished. Then, wetting experiments with indium were carried out for each of the three ceramic samples. As shown in Fig. 3, the wetting angles of indium with  $\text{Ti}_2\text{InC}$ ,  $\text{TiC}$ , and  $\text{SiC}$  ( $144.4^\circ$ ,  $155.7^\circ$ , and  $142.2^\circ$ , respectively) are large and quite close to one another, indicating the poor wettability between liquid indium and the three ceramics, which means a large interface energy. In addition, the incoherent metal-ceramic interface formed during the high-energy ball milling, which further increases the interfacial energy of the systems [39].

The thermal behaviors of the samples were investigated by DSC, as shown Fig. 4. The endothermic peak centered at  $156.61^\circ\text{C}$  can be indexed to the melting of indium, and appeared for all the three samples before ball milling treatment, indicating the existence of indium. After milling, the endothermic peaks for  $\text{TiC}$  and  $\text{SiC}$  samples are obviously depressed and broadened, as well as shifted left by  $5^\circ\text{C}$ , while the endothermic peak in  $\text{Ti}_2\text{InC}$  completely disappears. The broadening and left shift of the endothermic peak for the milled  $\text{SiC}$  and  $\text{TiC}$  samples can be explained as the small size effect and the increased interface energy stored during the high-energy ball milling treatment [39, 40].

More interface means more energy stored and the growth of more whiskers can be expected. To verify this deduction, we milled  $\text{Ti}_2\text{InC}$  with indium particles of different sizes (5 and  $20\ \mu\text{m}$ ). The two samples have the same  $\text{Ti}_2\text{InC}$ /indium mass ratio, and after the same ball milling treatment, more interface between  $\text{Ti}_2\text{InC}$  and indium would be formed in the sample with smaller indium particles. After incubation in the same conditions, as shown in Fig. 5, the much higher number density of whiskers in the sample with smaller indium is supportive of the mechanism that the interface energy drives the whisker growth.

Based on the discussion above, the driving force for the whisker growth process of the ball milling system can be ascribed to the interface energy. More surface energies stored during ball milling process result in

more whiskers formed in the later incubation stage. And the whisker growth propensity has a descending order of  $Ti_2InC$ ,  $TiC$  and  $SiC$ , consistent with the surface energy analysis for the three systems. In addition, the dependence of the whisker growth trend on the substrates can also be influenced by the crystalline structures of the substrates, as shown in the model in Fig. 6. Due to the layered structure of the  $Ti_2InC$ , the bonding between M and A atoms is weak, and it was calculated that the formation energy for indium vacancy is low (2.19 eV) [41], which means, for the indium atom diffusion, the indium atom planes of  $Ti_2InC$  phase can be a diffusion path in addition to the surfaces. In contrast, carbide ceramics are connected by covalent bonds, which have higher energy and are not easy to break, therefore, indium atoms can only diffuse along the surfaces of particles. Therefore, more indiums atoms can diffuse out of the pressed sample made from  $Ti_2InC$  than  $TiC$  and  $SiC$ .

## Conclusion

In this work, interface energy between indium and ceramic substrates as the driving force for metallic whisker growth was comparatively investigated. It was discovered for the first time that the systems of  $TiC/In$  and  $SiC/In$  have whisker growth after high-energy ball milling. Based on the interface energy and the difference in crystal structures of ceramic substrates, the whiskering propensities for the three systems of  $Ti_2InC/In$ ,  $TiC/In$  and  $SiC/In$  were discussed. The strongest propensity of indium whisker growth from  $Ti_2InC/In$  is ascribed to the higher interface energy in the system and the layered crystal structure of  $Ti_2InC$ . The finding of the contribution of the interface energy to the growth of whiskers will assist to comprehensively understand the long-awaited growth mechanism of metallic whiskers.

## Declarations

## Acknowledgements

This work was supported by the National Natural Science Foundation of China (No. 51731004), the National Key R&D Program of China (No. 2017YFE0301403), Natural Science Foundation of Jiangsu Province (BK20201283), and the Zhishan Youth Scholar Program of Southeast University.

## Funding

This work was supported by the National Natural Science Foundation of China (No. 51731004), the National Key R&D Program of China (No. 2017YFE0301403), Natural Science Foundation of Jiangsu Province (BK20201283), and the Zhishan Youth Scholar Program of Southeast University.

## Conflicts of interest/Competing interests

No conflict of interest exists in the submission of this manuscript, and the manuscript is approved by all authors for publication. I would like to declare on behalf of my co-authors that the work described is

original research that has neither been published nor is under consideration for publication in whole or in part elsewhere. All the authors listed have approved the manuscript that is enclosed.

### Availability of data and material

All data generated or analysed during this study are included in this published article.

### Code availability

Not applicable

## Relevance Summary

- a. It was discovered for the first time that the systems of TiC/In and SiC/In have whisker growth after high-energy ball milling.
- b. The strongest propensity of indium whisker growth from Ti<sub>2</sub>InC/In is ascribed to the higher interface energy in the system and the layered crystal structure of Ti<sub>2</sub>

## References

- [1] K. Compton, A. Mendizza, S. Arnold, *Corrosion* **7**, 327 (1951)
- [2] K. Chen, G.D. Wilcox, *Phys. Rev. Lett.* **94**, 066104 (2005)
- [3] J.D. Eshelby, *Phys. Rev.* **91**, 755 (1953)
- [4] K.N. Tu, *Phys. Rev. B* **49**, 2030 (1994)
- [5] M. Liu, J. Tao, C.Y. Nam, K. Kisslinger, L. Zhang, D. Su, *Nano Lett.* **14**, 5630 (2014)
- [6] A. He, D.G. Ivey, *J. Mater. Sci.* **50**, 2944 (2015)
- [7] Y. Liu, P. Zhang, L. Yang, W. Tian, Y. Zhang, Z. Sun, *Prog. Nat. Sci.* **28**, 569 (2018)
- [8] M.W. Barsoum, E.N. Hoffman, R.D. Doherty, S. Gupta, A. Zavaliangos, *Phys. Rev. Lett.* **93**, 206104 (2004)
- [9] M.W. Barsoum, T. El-Raghy, L. Farber, M. Amer, R. Christini, A. Adams, *J. Electrochem. Soc.* **146**, 3919 (1999)
- [10] M.W. Barsoum, *Prog. Solid State Chem.* **28**, 201 (2000)
- [11] Z.M. Sun, *Int. Mater. Rev.* **56**, 143 (2011)
- [12] M.W. Barsoum, M. Radovic, *Annu. Rev. Mater. Res.* **41**, 195 (2011)

- [13] C. Brüsewitz, I. Knorr, H. Hofsäss, M.W. Barsoum, C.A. Volkert, *Scr. Mater.* **69**, 303 (2013)
- [14] D. Wang, W. Tian, C. Lu, J. Ding, Y. Zhu, M. Zhang, P. Zhang, Z. Sun, *J. Alloys Compd.* **857**, 157588 (2020)
- [15] M. Imtyazuddin, A.H. Mir, M.A. Tunes, V.M. Vishnyakov, *J. Nucl. Mater.* **526**, 151742 (2019)
- [16] H. Fashandi, M. Dahlqvist, J. Lu, J. Palisaitis, S.I. Simak, I.A. Abrikosov, J. Rosén, L. Hultman, M. Andersson, A.L. Spetz, *Nat. Mater.* **16**, 814 (2017)
- [17] J. Ding, P. Zhang, W.B. Tian, J. Shi, M. Zhang, Y.M. Zhang, Z.M. Sun, *J. Alloys Compd.* **695**, 2850 (2017)
- [18] C.F. Hu, C. Li, J. Halim, S. Kota, D.J. Tallman, M.W. Barsoum, *J. Am. Ceram. Soc.* **98**, 2713 (2015)
- [19] Y. Liu, C. Lu, P. Zhang, J. Yu, Y. Zhang, Z.M. Sun, *Acta Mater.* **185**, 433 (2020)
- [20] P. Zhang, L.W. Shen, J. Ouyang, Y. Zhang, S. Wu, Z.M. Sun, *J. Alloys Compd.* **619**, 488 (2015)
- [21] M. Barsoum, L. Farber, *Science* **284**, 937 (1999)
- [22] T. El-Raghy, M. Barsoum, *Science* **285**, 1355 (1999)
- [23] E. Chason, N. Jadhav, F. Pei, E. Buchovecky, A. Bower, *Prog. Surf. Sci.* **88**, 103 (2013)
- [24] Y. Liu, P. Zhang, J. Yu, J. Chen, Y. Zhang, Z. Sun, *J. Mater. Sci. Technol.* **35**, 1735 (2019)
- [25] A. Kosinova, D. Wang, P. Schaaf, A. Sharma, L. Klinger, E. Rabkin, *Acta Mater.* **149**, 154 (2018)
- [26] D. Amram, O. Kovalenko, L. Klinger, E. Rabkin, *Scr. Mater.* **109**, 44 (2015)
- [27] J. Tang, P. Zhang, Y. Liu, C. Lu, Y. Zhang, W. He, W. Tian, W. Zhang, Z. Sun, *J. Mater. Sci. Technol.* **54**, 206 (2020)
- [28] C. Lu, Y. Liu, J. Fang, Y. Zhang, P. Zhang, Z. Sun, *Acta Mater.* **203**, 116475 (2021)
- [29] M.M. Ali, M.A. Hadi, I. Ahmed, A.F.M.Y. Haider, A.K.M.A. Islam, *Mater. Today Commun.* **25**, 101600 (2020)
- [30] J. Hu, H. Xiao, W. Guo, Q. Li, W. Xie, B. Zhu, *Ceram. Int.* **40**, 1065 (2014)
- [31] S. Haji Amiri, M. Ghassemi Kakroudi, T. Rabizadeh, M. Shahedi Asl, *Int. J. Refract. Met. Hard Mat.* **90**, 105232 (2020)
- [32] P. Zhang, Y. Zhang, Z. Sun, *J. Mater. Sci. Technol.* **31**, 675 (2015)

- [33] K. Suganuma, A. Baated, K.-S. Kim, K. Hamasaki, N. Nemoto, T. Nakagawa, T. Yamada, *Acta Mater.* **59**, 7255 (2011)
- [34] A. Baated, K.-S. Kim, K. Suganuma, *J. Mater. Res.* **25**, 2175 (2010)
- [35] W. Shim, J. Ham, K.-i. Lee, W.Y. Jeung, M. Johnson, W. Lee, *Nano Lett.* **9**, 18 (2009)
- [36] D. Pradhan, S. Panda, L.B. Sukla, *Miner. Process Extr. Metall. Rev.* **39**, 167 (2018)
- [37] S. Li, G. Bei, H. Zhai, Z. Zhang, Y. Zhou, C. Li, *J. Mater. Res.* **22**, 3226 (2007)
- [38] Y. Liu, P. Zhang, Y.M. Zhang, J. Ding, J.J. Shi, Z.M. Sun, *Mater. Lett.* **178**, 111 (2016)
- [39] P.-L. Sun, S.-P. Wu, S.-C. Chang, T.-S. Chin, R.-T. Huang, *Mater. Sci. Eng. A* **600**, 59 (2014)
- [40] C. Koch, J. Jang, S. Gross, *J. Mater. Res.* **4**, 557 (1989)
- [41] B. Liu, J.Y. Wang, J. Zhang, J.M. Wang, F.Z. Li, Y.C. Zhou, *Appl. Phys. Lett.* **94**, (2009)

## Figures

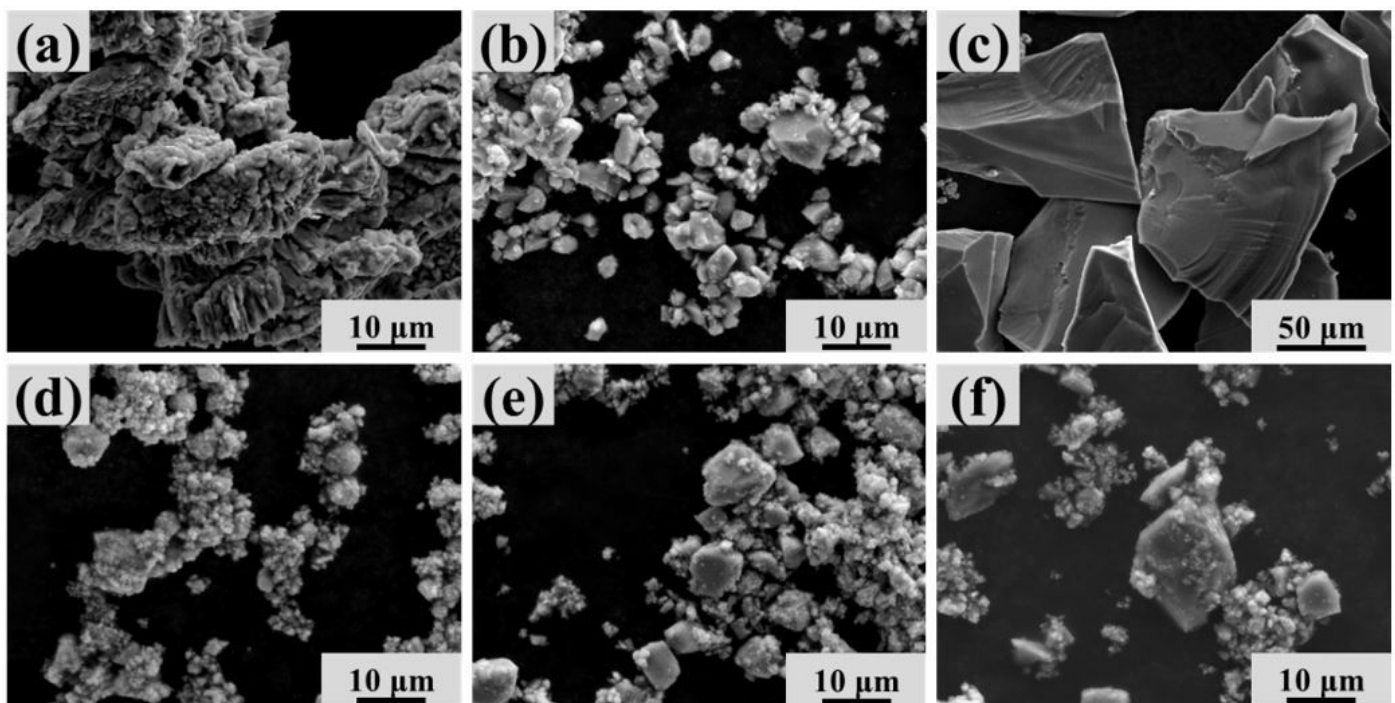


**Figure 1**

SEM images. The as-synthesized  $\text{Ti}_2\text{InC}$  (a), the as-purchased  $\text{TiC}$  (b) and  $\text{SiC}$  (c); the ball-milled  $\text{Ti}_2\text{InC}$  (d),  $\text{TiC}$  (e) and  $\text{SiC}$  (f).

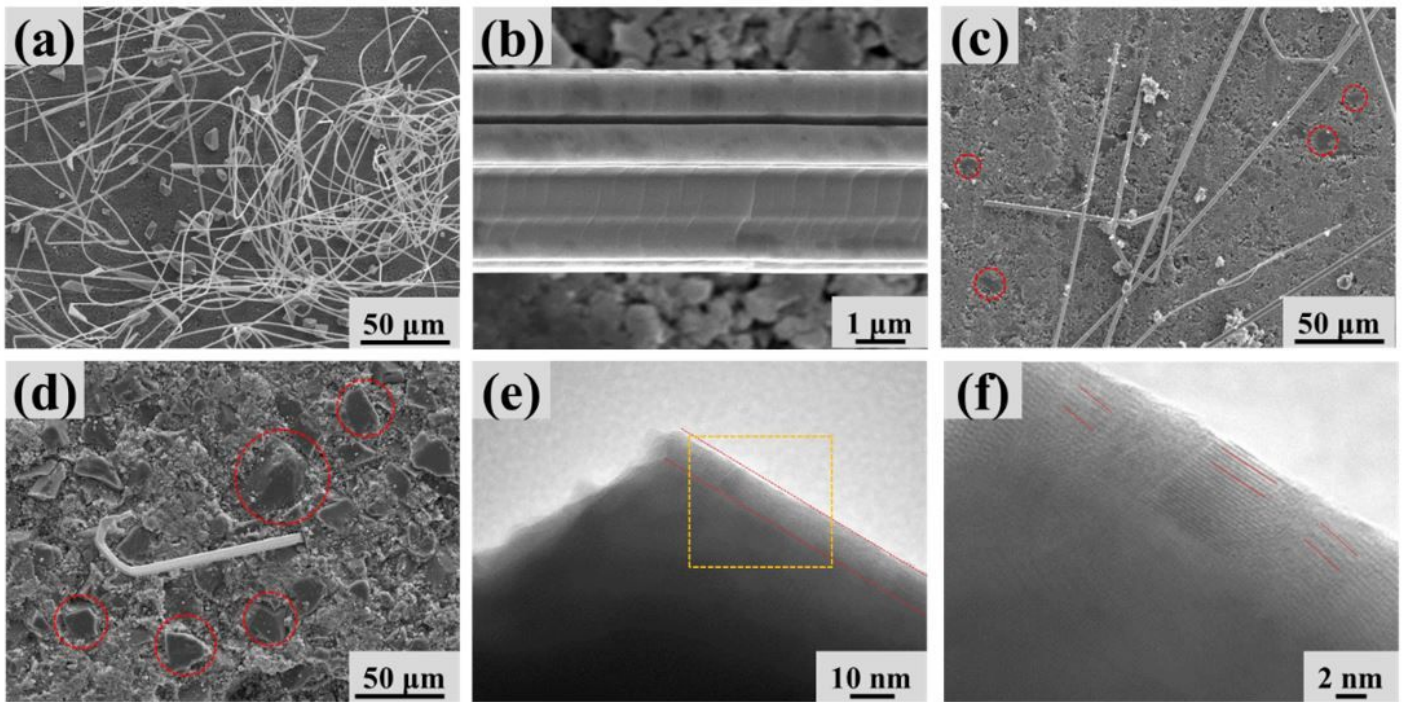


**Figure 2**

Whisker growth on samples Ti<sub>2</sub>InC/0.1In (a)&(b), TiC/0.1In (c) and SiC/0.1In (d). TEM images of indium whiskers (e) and magnified view of yellow rectangle area (f).

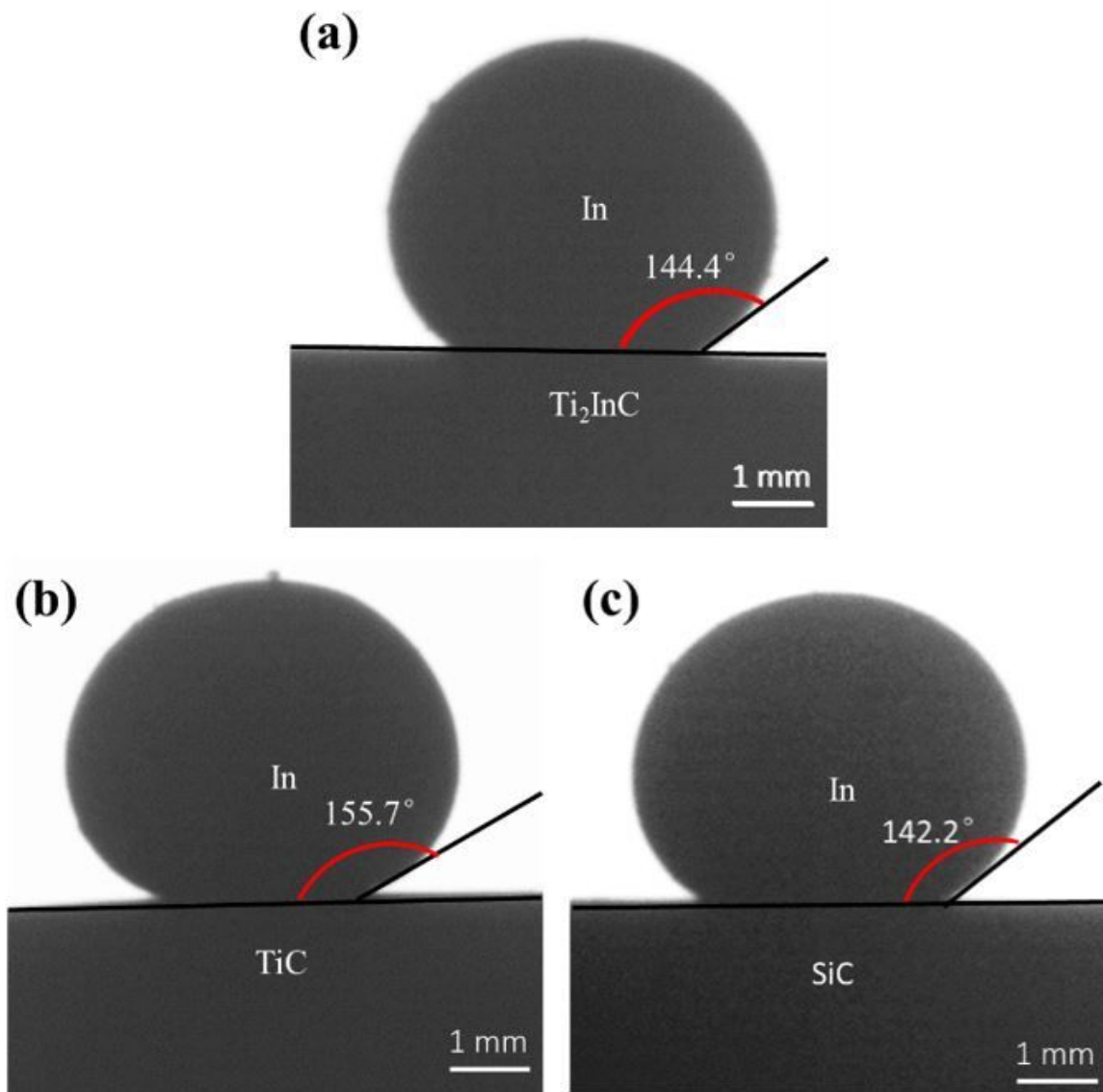


**Figure 3**

Contact angles between liquid indium and  $Ti_2InC$  (a),  $TiC$  (b) and  $SiC$  (c).

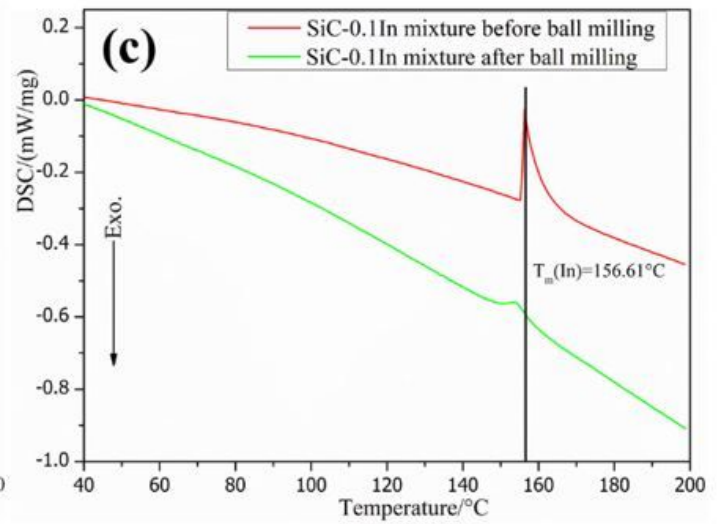
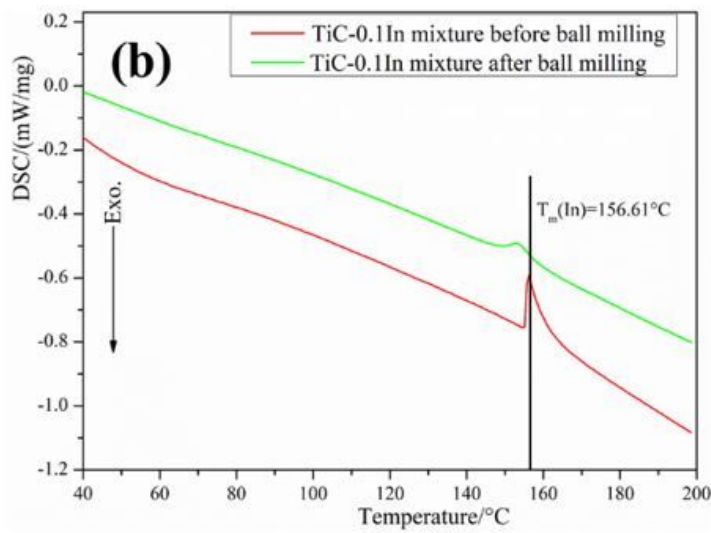
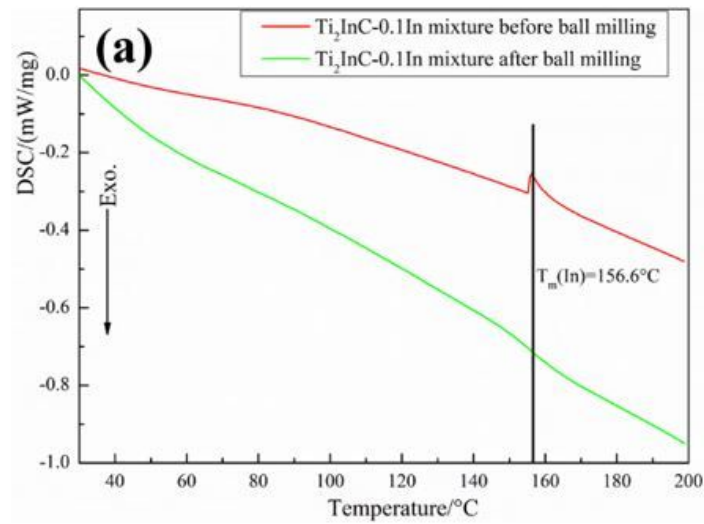


**Figure 4**

DSC curves for the samples of  $\text{Ti}_2\text{InC}/0.1\text{In}$  (a),  $\text{TiC}/0.1\text{In}$  (b) and  $\text{SiC}/0.1\text{In}$  (c) before and after ball milling treatment.

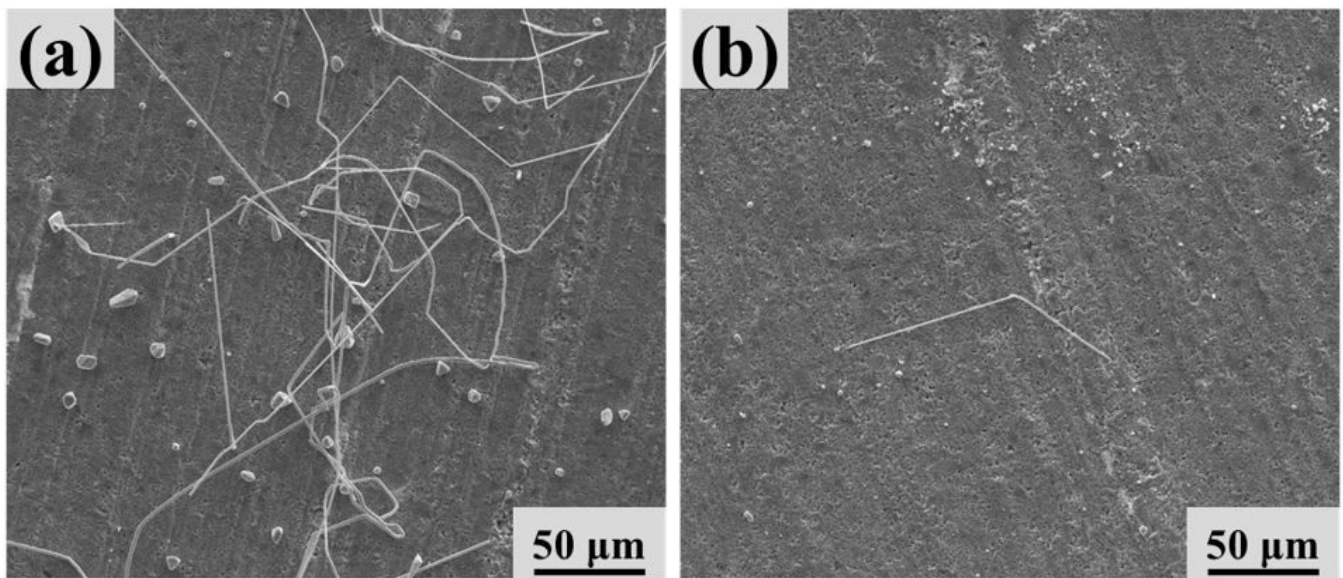


**Figure 5**

Number densities of the indium whiskers on the samples of milled  $\text{Ti}_2\text{InC}$  and indium particles. (a) indium particles of  $5\ \mu\text{m}$ , and (b) indium particles of  $20\ \mu\text{m}$ .

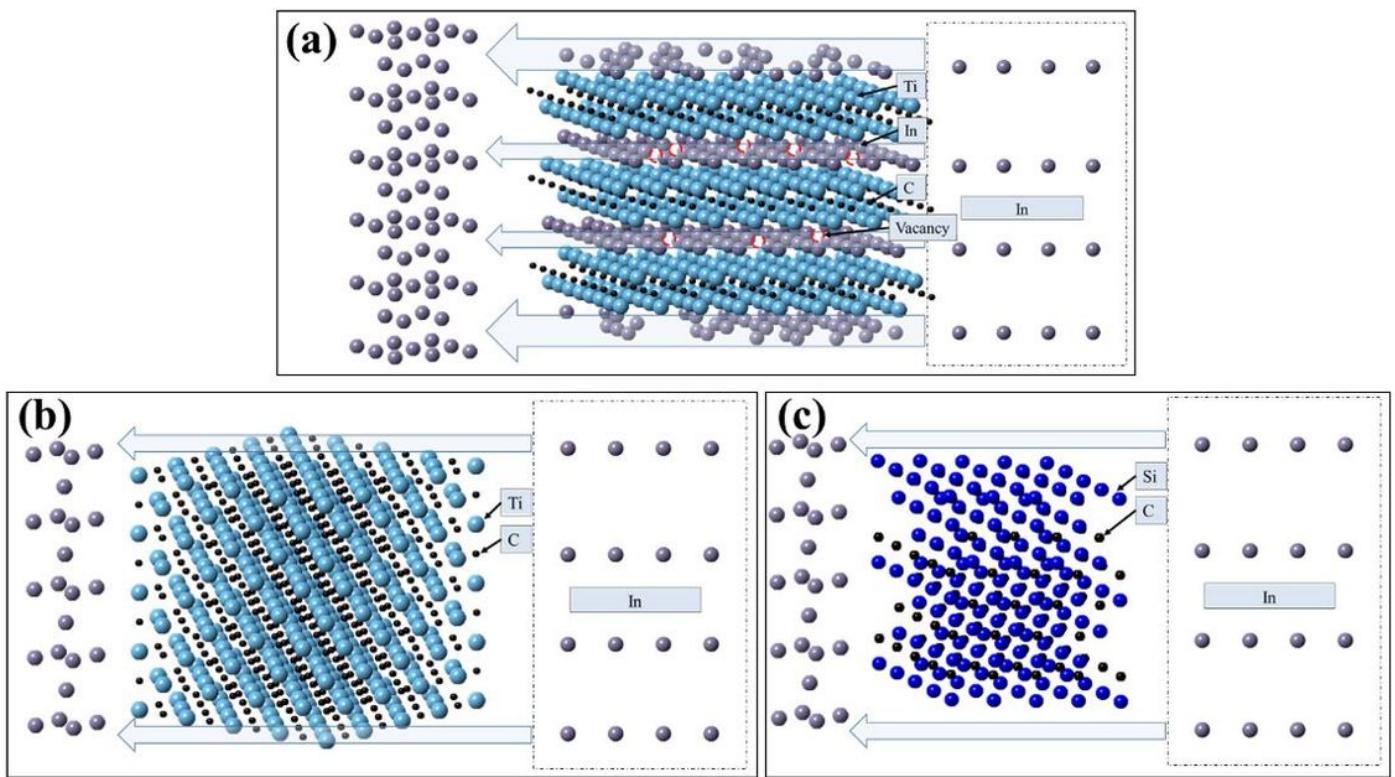


**Figure 6**

Schematic diagram of whisker growth in  $\text{Ti}_2\text{InC}/0.1\text{In}$  (a),  $\text{TiC}/0.1\text{In}$  (b) and  $\text{SiC}/0.1\text{In}$  (c).